Contract NAS9-14126
DRL T-960
L.I. 5
DRD MA-129T

HIGH PERFORMANCE N_2O_4/AMINE ELEMENTS
FINAL SUMMARY REPORT

March 1976

(NASA-CR-147572) HIGH PERFORMANCE N2O4/AMINE ELEMENTS Final Summary Report (Rocketdyne) 53 p HC $4.50 CSCL 21I

N76-22401

Unclas
G3/28 27655

by

A. Y. Falk

Prepared for

National Aeronautics and Space Administration
Lyndon B. Johnson Space Center

ROCKWELL INTERNATIONAL/ROCKETDYNE DIVISION
6633 Canoga Avenue
Canoga Park, California

Contract NAS9-14126
DRL T-960
L.I. 5
DRD MA-129T
Rocketdyne R-9847-2

HIGH PERFORMANCE N_2O_4/AMINE ELEMENTS
FINAL SUMMARY REPORT

March 1976

Prepared by

A. Y. Falk

Approved by

W. H. Nurick
Program Manager
Combustion Programs

Prepared for

National Aeronautics and Space Administration
Lyndon B. Johnson Space Center

ROCKWELL INTERNATIONAL/ROCKETDYNE DIVISION
6633 Canoga Avenue
Canoga Park, California

FOREWORD

This report was prepared for the NASA Lyndon B. Johnson Space Center, Houston, Texas by the Advanced Programs Department of Rocketdyne Division, Rockwell International. The study was conducted in accordance with Contract NAS9-14126, Rocketdyne G.O. 09640. Mr. M. F. Lausten of the Lyndon B. Johnson Space Center served as the NASA Technical Manager. The Rocketdyne Program Manager was Mr. W. H. Nurick.

The work conducted on this contract is described in greater detail in Rocketdyne Report R-9847-1.

ABSTRACT

An analytical and experimental investigation was conducted to develop an understanding of the mechanisms that cause reactive stream separation, commonly called "blowapart," for hypergolic propellants. The investigation was limited to the N_2O_4/MMH propellant combination and to a range of engine-operating conditions applicable to the Space Tug and Space Shuttle attitude control and orbital maneuvering engines. Primary test variables were: chamber pressure (1 to 20 atm), fuel injection temperature (283 to 400^{o}K)m and propellant injection velocity (9 to 50 m/s). The injector configuration studied was the unlike doublet. The reactive stream separation experiments were conducted using special combustors designed to permit photography of the near-injector spray combustion flow field. Analysis of color motion pictures provided the means of determining the occurrence of reactive stream separation.

Through a basic understanding of the governing mechanisms, meaningful design criteria were established which defined regions of operation that are free from reactive stream separation for N_2O_4/MMH propellants.

CONTENTS

PRECEDING PAGE BLANK NOT FILMED

ILLUSTRATIONS

TABLES

1.0 INTRODUCTION

1.1 OBJECTIVE

The objective of this program was to develop an understanding of the mechanisms that cause reactive stream separation (RSS), commonly called "blowapart", for hypergolic propellants. Through a basic understanding of the governing mechanisms, design criteria were to be established which would allow the design of stable high performing injectors that are free from RSS and "pops" (cyclic blowapart).

1.2 BACKGROUND

Hypergolic earth-storable propellants such as N_2O_4/amine-type fuels are prime candidates for use on the Space Shuttle attitude control and orbital maneuvering engines (OME) as well as for Space Tug applications. These types of hypergolic propellants, being highly reactive, can experience reactive stream separation and/or cyclic blowapart (popping) under some conditions. The former is a quasi steady-state phenomenon that, for impinging jet injector designs, turns the propellant streams away from each other so that intra-element propellant mixing is impaired. This causes poor overall propellant mixing uniformity and thereby, results in lowered combustion efficiency. Cyclic blowapart (or popping) is caused by small explosions that occur in the spray mixing region. These explosions or "pops" can sustain and/or drive acoustic instabilities as well as result in cyclic disruption of the mixing process which can lower the overall time averaged combustion efficiency. Because of the extremely high combustion efficiencies and reliability required for current applications, it is imperative that the cyclic blowapart and reactive stream separation phenomenon be understood and their undesirable effects be minimized.

Over the past 15 years, numerous studies have been conducted in efforts to identify the reactive stream separation and/or popping operating limits

as well as to develop injector design criteria for their avoidance. Examples of some of these studies are those of Refs. 1 through 24. Both RSS and popping have been experimentally observed and several physical models postulated. Unfortunately, none of the existing models can to date account for all of the experimentally determined RSS or popping. Existing models give satisfactory correlation of only selected sets of available experimental data. This defect is due to a lack of a clear understanding of the physical/chemical processes controlling the various phenomena as well as the interaction of competing mechanisms. Meaningful rocket engine design criteria that will ensure blowapart-free operation can result only from determination of: (1) the explosion and separation mechanisms, and (2) their relationship to engine operating conditions and injector design specifications. A survey of existing information provided the background for this study.

1.3 SCOPE

This investigation was limited to the N_2O_4/MMH propellant combination and to a range of engine operating conditions applicable to the Space Tug and Space Shuttle attitude control and orbital maneuvering engines as defined in Table 1-1. The injector configurations studies were single-element unlike doublets.

TABLE 1-1. RANGE OF COMBUSTION OPERATING CONDITIONS FOR INVESTIGATION

Chamber pressure	4 to 20 atm	(60-300 psia)
Mixture ratio	1.6 to 2.2	
Fuel temperature	277 to 394°K	(40 to 250°F)
Oxidizer temperature	277 to 339°K	(40 to 150°F)
Minimum orifice diameter	0.0508 cm	(0.020-inch)
Maximum orifice diameter	0.1016 cm	(0.040-inch)
Injection ΔP	0.7 to 17 atm	(10 to 250 psi)

Hot-fire testing and analyses were conducted to establish meaningful design criteria for stable high performing injectors that are free from pops and RSS.

2.0 SUMMARY

The objective of this program was to develop an understanding of the mechanisms that cause reactive stream separation, commonly called "blowapart", for hypergolic propellants. Analytical and experimental investigations were conducted to accomplish this objective. The study was limited to the N_2O_4/MMH propellant combination and to a range of engine operating conditions applicable to the Space Tug and Space Shuttle attitude control and orbital maneuvering engines.

Primary test variables were: chamber pressure (1 to 20 atm; 13.7 to 300 psia), fuel injection temperature (283 to 400°K; 50 to 260°F), and propellant injection velocity (9 to 50 m/s; 30 to 160 ft/sec). Nominal mixture ratio for all tests was $\sim$1.7, the equal volume value for the N_2O_4/MMH propellant combination. The injector configuration studied was the unlike doublet. The reactive stream separation experiments were conducted using special combustors designed to permit photography of the near-injector spray combustion flow field. Analysis of the color motion pictures provided the means of determining the occurrence of reactive stream separation.

Two types of reactive stream separation, with different driving mechanisms, were observed during the conduct of the program. One of them, termed penetration, occurred at high injection velocities and/or chamber pressures with ambient or moderately heated (fuel) propellants. The other phenomena, termed separation, occurred at elevated fuel temperatures. Through a basic understanding of the governing mechanisms, design criteria were established which defined regions of operation that are free from reactive stream separation for N_2O_4/MMH propellants.

To prevent penetration, the design criteria established was that the fuel stream Weber number be less than 14. That is

$$\boxed{\text{Weber Number} = \frac{\rho_g \, v_f^2 \, d_f}{\sigma_f \, g_c} < 14}$$

To prevent separation, which can occur with heated propellants, the injector design should be based on the following criteria

$$\boxed{\frac{x_c}{L_c} = \frac{1}{\Delta EA} \, e^{\Delta E/R_g T_o} \left[\frac{v_f \, T_o^3 \, C_p \, \rho_\ell \, R_g^2}{C_4 \, P \, \Delta H} \right]}$$

where

$$\frac{x_c}{L_c} < 1 \quad \text{gives separation}$$

$$\boxed{\frac{x_c}{L_c} > 1 \quad \text{gives mixing}}$$

$$\frac{x_c}{L_c} = 1 \quad \text{is the boundary between separation and mixing}$$

The value of all quantities required to calculate x_c/L_c are known. Evaluation of the constants C_4, A, and ΔE were determined by correlation of the experimental data. The design criteria were based on the experimental data of this contract (NAS9-14126) and a related effort conducted by Aerojet (NAS9-14186).

3.0 RELATED NASA STUDY

Concurrent with the investigation conducted by Rocketdyne, Aerojet Liquid Rocket Company conducted a related effort on NASA Contract NAS9-14186 (Ref. 26).

Aerojet conducted approximately 90 tests employing N_2O_4/MMH with an element similar in design to the UD-1 element employed in this study. During that investigation, chamber pressure was varied from an absolute pressure of 5.4 to 68 atm (80 to 1000 psia), fuel injection temperature from 277 to 422^oK (40 to 300^oF), oxidizer injection temperature from 283 to 338^oK (50 to 150^oF), and propellant injection velocities from $\sim$9 to 55 m/s (30 to 180 ft/sec). Nominal mixture ratio for all was $\sim$1.7. Consequently, in addition to conducting tests over the same range of test conditions as on this contract, Aerojet conducted tests at higher injection velocities, chamber pressure, and fuel temperature with the UD-1 element.

Several important differences in the experimental test setup and/or data interpretation between this study and Aerojet's should be noted. Whereas Rocketdyne employed only backlighting of the spray field, Aerojet utilized one lamp to backlight the spray area and with second and third lamps provided top and front lighting. Rocketdyne employed only backlighting because previous experience (Ref. 11, 13, and 21) had indicated that this was the most effective means of lighting for definition of mixed versus separated/penetrated test conditions. Separation/penetration being defined as a clearly defined separation of the spray fan downstream of the jet impingement point. Aerojet (Ref. 26), on the other hand, appears to define separation and/or penetration as the appearance of unmixed propellants in the spray field evidenced by color differences between the fuel and oxidizer. Energetic cyclic blowapart (i.e., popping) was not observed on any of the tests conducted by Aerojet or Rocketdyne.

The data from both Contract NAS9-14186 and this program (Contract NAS9-14126) are correlated and design criteria are established which will allow for the design of stable high-performing injectors that are free from reactive stream separation (Section 5.0).

4.0 EXPERIMENTAL CONSIDERATIONS

The test facility, experimental hardware, photographic technique employed, and experiments conducted are briefly described herein.

4.1 TEST FACILITY

The reactive stream separation experiments were performed on test stand Victor in the Propulsion Research Area (PRA) of Rocketdyne's Santa Susana Field Laboratory (SSFL) using special combustors designed to permit photography of the near-injector spray combustion flow field.

Victor test stand, as used in the hot firing experiments, is shown schematically in Fig. 4-1. Note that to permit variation of chamber pressure at fixed propellant injection conditions (i.e., flowrate, injection velocity, etc.), a regulated gaseous nitrogen (GN_2) combustion chamber bleed system was employed in conjunction with a fixed combustor throat area. Regulation of the GN_2 flowrate in conjunction with the propellant flowrates made it possible to vary chamber pressure at fixed injection conditions. The GN_2 bleed provided most of the desired combustion chamber pressure.

4.2 HARDWARE

The experimental hardware consisted of two basic components: (1) an injector assembly, and (2) a combustion chamber assembly. The injector assembly contained two separately manifolded unlike-doublet elements. Two different combustion chamber assemblies, both of which permitted pictures to be taken of the doublet spray pattern, were employed.

4.2.1 Combustion Chamber

Two combustion chamber assemblies of different design were employed. One of these was a high contraction ratio (ε_c = 77) tapered chamber. The other was a low contraction ratio (ε_c = 12) cylindrical chamber.

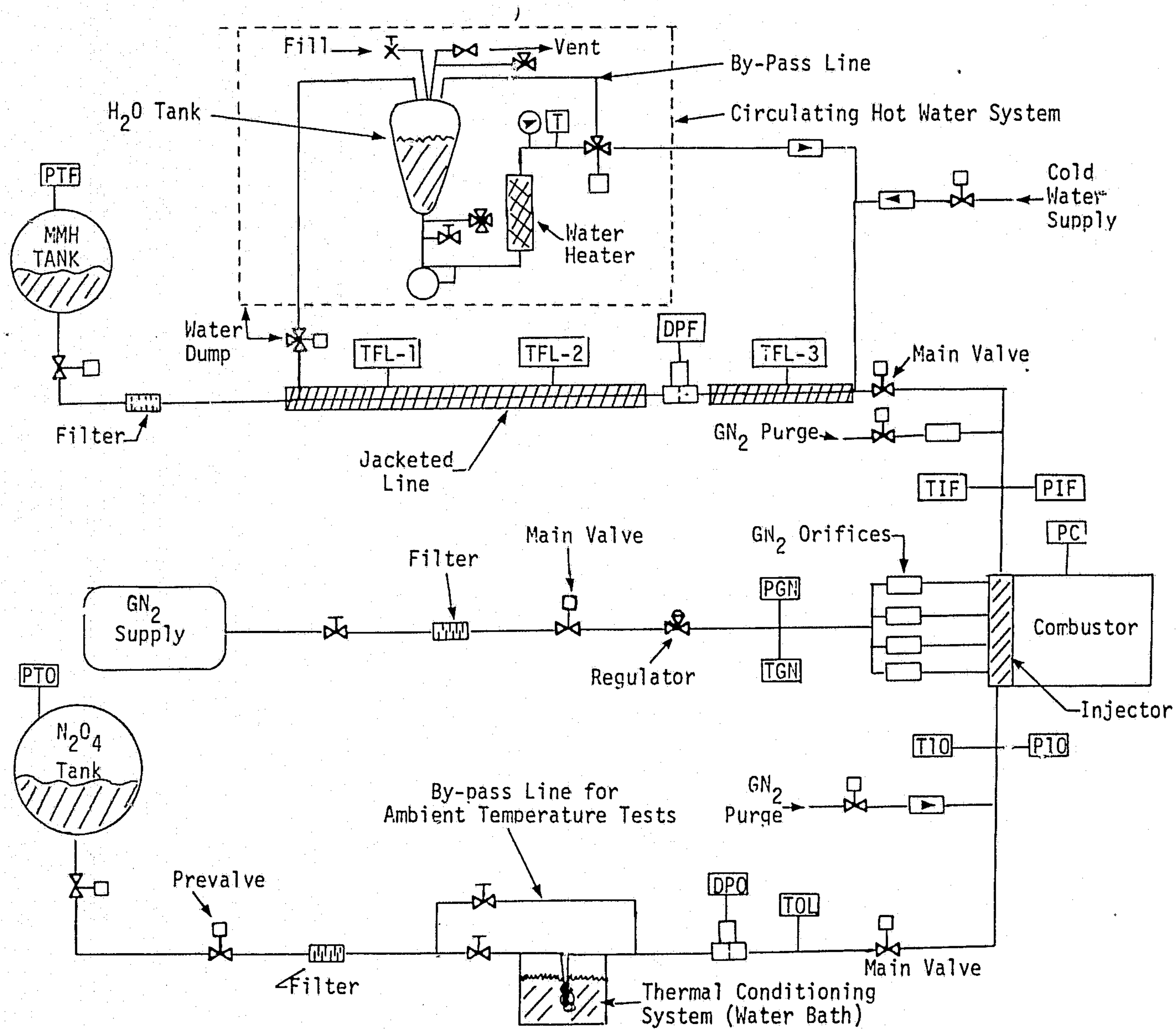

Figure 4-1. Schematic of Test Stand Used for Hot-Firing Experiments (Victor Stand PRA)

Schematics of the tapered and cylindrical chambers are presented as Figs. 4-2 and 4-3, respectively. Both chambers employed the same basic injector assembly and had the same throat area (~5 cm^2; 0.77 $in.^2$). Minor modification of the injector assembly was necessary to adapt the injector to the low contraction ratio chamber after its initial use in the high contraction rate chamber.

The design of the initial (high contraction ratio) chamber was based upon hardware previously employed at Rocketdyne (Ref. 21) and incorporated the following features:

1. Two viewing windows located diametrically opposite each other so as to permit pictures to be taken of the doublet spray pattern.
2. Capability to vary chamber pressure independent of propellant injection rate by variation of a GN_2 base bleed flowrate.
3. Use of the GN_2 bleed to protect both the windows and combustor walls from hot combustion gases, permitting repeated tests of any desired duration in an economical and otherwise uncooled system.
4. The GN_2 bleed (which had flowrates from 10 to 30 times the injected propellant flows) was expected to sweep away unreacted spray or recirculating N_2O_4 vapors which had previously interferred with photographic studies in high contraction ratio chambers.

This latter feature did not work well inthe high contraction ratio chamber. Consequently, a low contraction ratio cylindrical chamber was designed and employed for the latter portion of the hot-fire testing.

The high contraction ratio tapered chamber was employed for the first 199 tests. Satisfactory movies of the impinging streams were not obtained for many of these tests because of gross recirculation which occurred in the

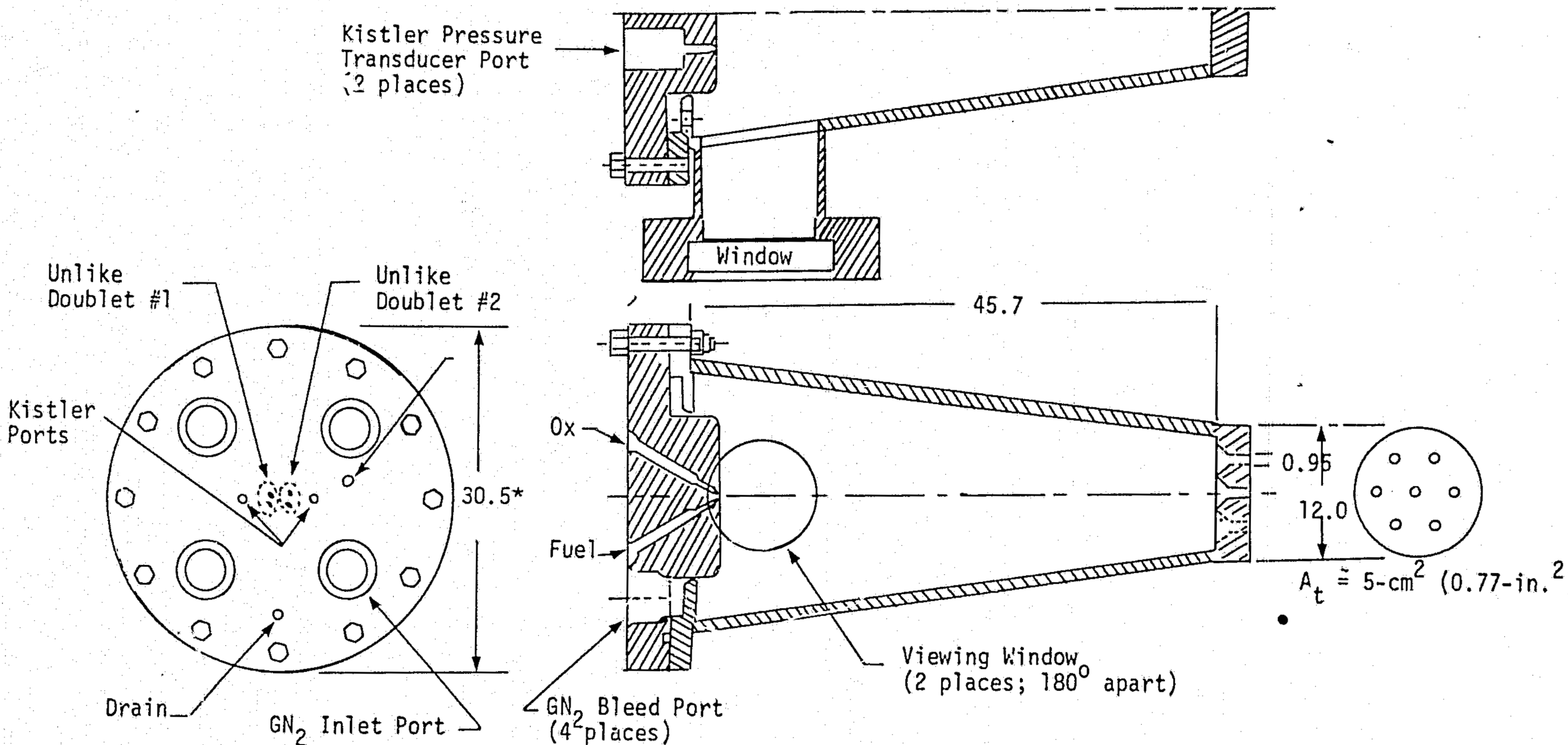

*Dimensions are in centimeters

Figure 4-2. Schematic Illustration of High Contraction Ratio Tapered Combustor Assembly

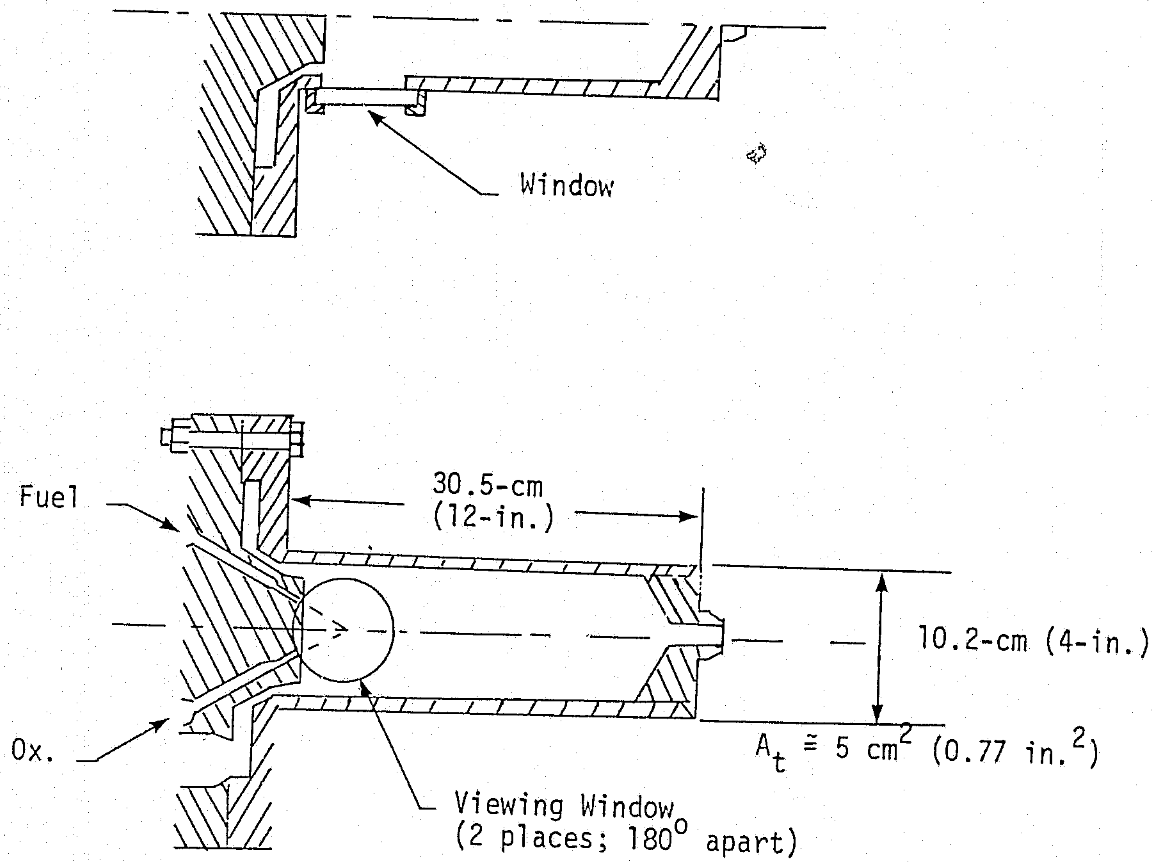

Figure 4-3. Schematic Illustration of Low Contraction Ratio Cylindrical Combustor Assembly

combustor. N_2O_4/combustion products obstructed the view of the impinging streams for many of these tests. To overcome this difficulty, the chamber (combustor) design was revised to suppress recirculation and, thereby, permit better photographs to be taken of the impinging streams. The chamber volume (diameter and length) was reduced and the viewing windows were mounted essentially flush rather than recessed (see Figs. 4-2 and 4-3). This design proved to be better for obtaining the desired movies of the hot-firing experiments.

The low contraction ratio chamber incorporates the same basic features as the high contraction ratio chamber. However, there are several significant differences in design:

1. The chamber has a lower contraction ratio (~12 rather than ~77) and is cylindrical rather than tapered.
2. The viewing windows are mounted nearly flush to the chamber wall rather than being recessed ~10 cm (4-inch).

The lower contraction ratio and flush mounting of the viewing windows are believed to be the major reasons for reduced recirculation and thereby, increased ability to obtain better pictures of the impinging streams with this chamber assembly.

4.2.2 Injector

The injector contained two separately-manifolded unlike-doublet elements, the impingement points of which are located on the horizontal centerline of the chamber approximately 0.9525-cm (0.375-inch) to either side of the vertical centerline. The individual doublets have the specifications presented in Table 4-1. Rounded orifice entrances were employed such that the doublet elements would exhibit stable coherent jet characteristics. Only one doublet was connected during a given test.

TABLE 4-1. UNLIKE-DOUBLET ELEMENT CONFIGURATIONS

Element Designation	Fuel Orifice Diameter		Oxidizer Orifice Diameter		Impingement Angle, Degrees	Orifice L/D	Impingement Distance, L/D
	cm	Inch	cm	Inch			
UD-1	0.0508	0.020	0.061	0.024	60	12	~6
UD-2	0.0838	0.033	0.1016	0.040	60	12	~6

4.3 PHOTOGRAPHY

Motion pictures were taken of the doublet spray fan during each test using either a Millikan DBM 50AM camera at ~400 frames/sec or a Fastax at ~4000 frames/sec. In general, the lower frame speed was employed to reduce costs. Use of the lower speed film made it possible to conduct more tests in any given test slot. Fastax movies were taken in regions where cyclic "blowapart" was observed to better define the phenomenon. Eastman Kodak Ektachrome EF color film was employed for the first 158 tests and EFB color film was used for the remaining 113 experiements. The EF film is sensitive to daylight (sunlight) whereas EFB film is sensitive to a tungsten filament lamp. Back-light illumination was provided by a GE model BFJ 750 watt tungsten filament lamp and focused by a Fresnel lens at the photochamber window opposite the camera. A schematic of the photographic test setup is presented in Fig. 4-4. All photographs were taken with the camera looking "edgewise" through the doublet spray fan.

4.4 HOT-FIRE EXPERIMENTS

4.4.1 Tests Conducted

A total of 271 hot firing N_2O_4/MMH experiments were conducted; however, only 163 of these tests provided meaningful data in terms of reactive stream separation. Unsatisfactory films were obtained on a number of tests because recirculating N_2O_4 fumes and/or combustion gas products

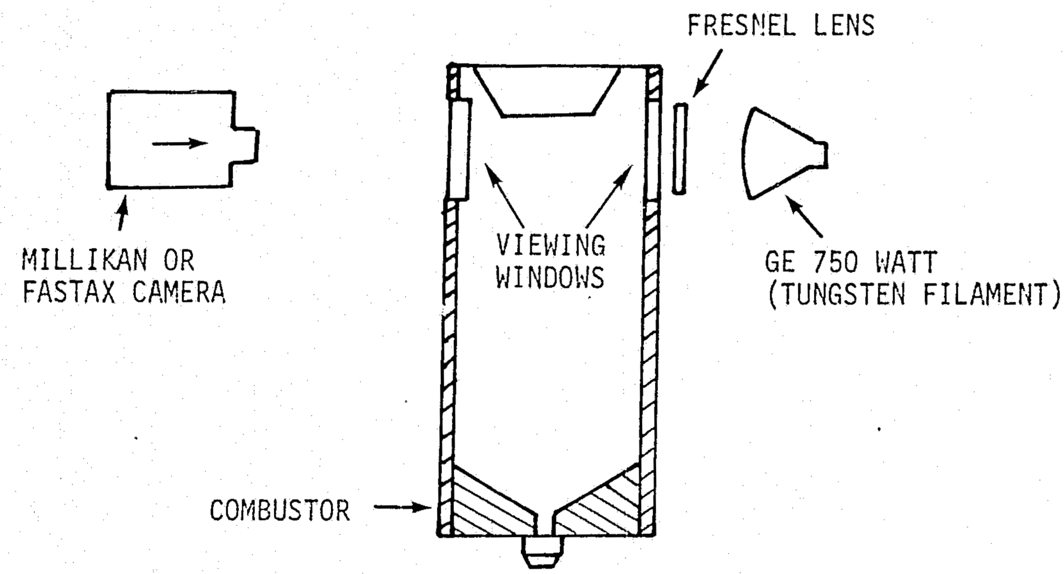

Figure 4-4. Schematic of Photographic Test Setup

obscured the view of the spray fan. As noted above, a modification of the chamber design was made to resolve this problem in the latter part of the program. The first 199 tests were conducted using the original high contraction ratio tapered chamber and the final 72 tests were conducted in a lower contraction ratio cylindrical chamber. The second (low contraction ratio) chamber design resolved the chamber gas recirculation problem.

The majority of the tests (202 of 271) were conducted utilizing the UD-2 element. During these tests, chamber pressure was varied from an absolute pressure of 0.94 to ~15 atm (13.7 to 220 psia), fuel injection temperature from 283 to 400^{o}K (50 to 260^{o}F), and oxidizer injection temperature from 283 to 322^{o}K (50 to 120^{o}F). Propellant injection velocities were varied from ~9 to 50 m/sec (30 to 160 ft/sec). Tests conducted with the UD-1 element covered a smaller range of fuel injection velocity (~9 to 25 m/s; 30 to 80 ft/sec) and fuel injection temperature (283 to 350^{o}K; 50 to 170^{o}F). Nominal mixture ratio for the majority of the tests was ~1.7 (the equal volume value for the N_2O_4/MMH propellant combination).

4.4.2 Occurrence of Separation

Analysis of the color motion pictures provided the means of determining the occurrence of reactive stream separation. The readability of the films were divided into five categories: excellent, good, satisfactory, marginal, and unsatisfactory.

The tests in which marginal or better films were obtained were divided into several categories: mixed, separated, penetrated, or a combination of the above. Mixed tests were those in which no reactive stream separation was apparent. Two different types of reactive stream separation phenomenon were observed. One of these, termed penetration, was observed at high injection velocities with ambient temperature propellants. In this case, a portion of the fuel stream appeared to penetrate through or go around the oxidizer stream. The other phenomena, termed separation, was observed with heated propellants.

The fuel and oxidizer streams appeared to blowapart and/or separate starting at some point downstream of the impingement point and progress backward to the impingement point when this phenomena was observed. In both cases, the observed reactive stream separation phenomena consisted of repeated pulses (i.e., it was cyclic). However, the pulsing did not exhibit the strength necessary to either disrupt the doublet jets upstream of the impingement point or to completely destroy the spray fan downstream of the impingement point; i.e., there were no instances of energetic stream blowapart or "popping" observable in the film data.

It should be noted that many of the tests where reactive stream separation was observed a clear distinction could not be made as to whether the phenomena was "separation" or "penetration". Since the two phenomenon appear to be driven by different mechanisms, the basis of selection for terminology was based on whether the tests were conducted at high injection velocity (termed penetration) or with heated fuel (termed separation). The method of selection of the category (mixed, separated, or penetrated) is qualitative and subjective. Consequently, in some cases a combined result such as mixed/separated or separated/penetrated was reported.

Photographs of two tests, one mixed and one penetrated, are presented in Fig. 4-5 to illustrate the phenomenon observed. The test number and test conditions are noted on the figure.

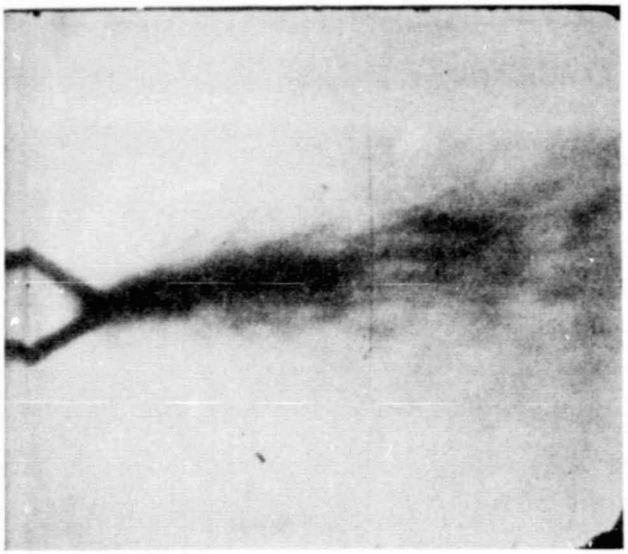

Test No. - 51

Element - UD-2

P_c - 0.429×10^6 N/M^2 (62 psia)

V_f - 13.7 m/s (45 ft/sec)

T_f - 324^{o}K (124^{o}F)

A. Mixed Test Condition

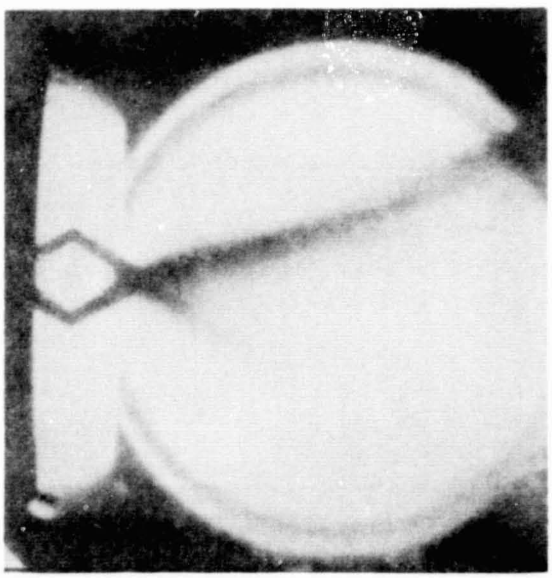

Test No. - 203

Element - UD-2

P_c - 0.782×10^6 N/M^2 (113 psia)

V_f - 30.2 m/s (99 ft/sec)

t_f - 293^{o}K (68^{o}F)

B. Penetrated Test Condition

Figure 4-5. Typical Photographs of Mixed and Penetrated Test Conditions

5.0 DISCUSSION OF RESULTS

A discussion and correlation of the experimental results from this program (Contract NAS9-14126) and the concurrent related effort conducted by Aerojet (Contract NAS9-14186) are presented herein.

5.1 DATA CORRELATION

Two different types of reactive stream separation, with different driving mechanisms, appear to have been observed during the conduct of the subject contracts. One of these occurs at high injection velocities and/or chamber pressures with ambient temperature or moderately heated propellants. The other, occurs at elevated propellant (fuel) temperatures. Development of models to predict test conditions which will not result in the occurrence of reactive stream separation by either of the two phenomenon are presented in the following paragraphs. These models can be employed as guidelines in the design of stable, high-performing injectors free from reactive stream separation.

5.1.1 Impinging Jet Characteristics Model

A model (termed Impinging Jet Characteristics Model) to characterize the ambient temperature or moderately heated propellants reactive stream separation phenomena was developed based on Rocketdyne's data on the UD-1 and UD-2 elements and Aerojet's UD-1 element data. As was noted in Section 4.0, Rocketdyne observed what is termed "penetration" at the higher injection velocities and chamber pressures with the UD-2 element. Similarly, Aerojet observed what it called "separation" at the higher injection velocities and chamber pressures with the UD-1 element.

Plots of chamber pressure versus fuel injection velocity for the UD-1 and UD-2 elements are presented as Figs. 5-1 and 5-2, respectively. A distinction as to whether each test was mixed, separated, penetrated, etc., is made in the figures. In addition, a differentiation between Rocketdyne and Aerojet data is made in Fig. 5-1. With the exception of whether the UD-1 element is mixed or penetrated at low injection velocities, Rocketdyne's and Aerojet's data are consistent (Fig. 5-1). The similarity between the data plots for the UD-1 and UD-2 elements should be noted. Both predict reactive stream separation at the higher injection velocities in combination with higher chamber pressures. Rocketdyne called the phenomena penetration (Fig. 5-2), while Aerojet termed it separation; however, both agree that some form of reactive stream separation occurs at the higher injection velocities in combination with higher chamber pressures. Separated, penetrated, and mixed regions are noted on the figures. Reactive stream separation occurs at lower injection velocities and chamber pressures with the larger element (UD-2).

It should be noted that only tests conducted with fuel injection temperatures less than the value required for separation due to fuel temperature effects ($T_f < 338^oK$ for the UD-1 element and less than 316^oK for the UD-2 element) are shown in Figs. 5-1 and 5-2. Definition of these temperature limits is established later. This was necessary to avoid the confusion of showing separated conditions at low injection velocity that were due to fuel temperature effects and not injection velocity effects.

As was initially suggested by Aerojet (Ref. 26), the penetration/separation which occurs at higher injection velocities and chamber pressures can be related to the Weber number of the impinging jets. This is illustrated in Figs. 5-3 and 5-4 in which chamber pressure is plotted versus the fuel stream Weber number for the UD-1 (Fig. 5-3) and UD-2 (Fig. 5-4) elements. Both Rocketdyne and Aerojet data are presented in these figures. As was the case in Figures 5-1 and 5-2, the Rocketdyne and Aerojet data are consistent with

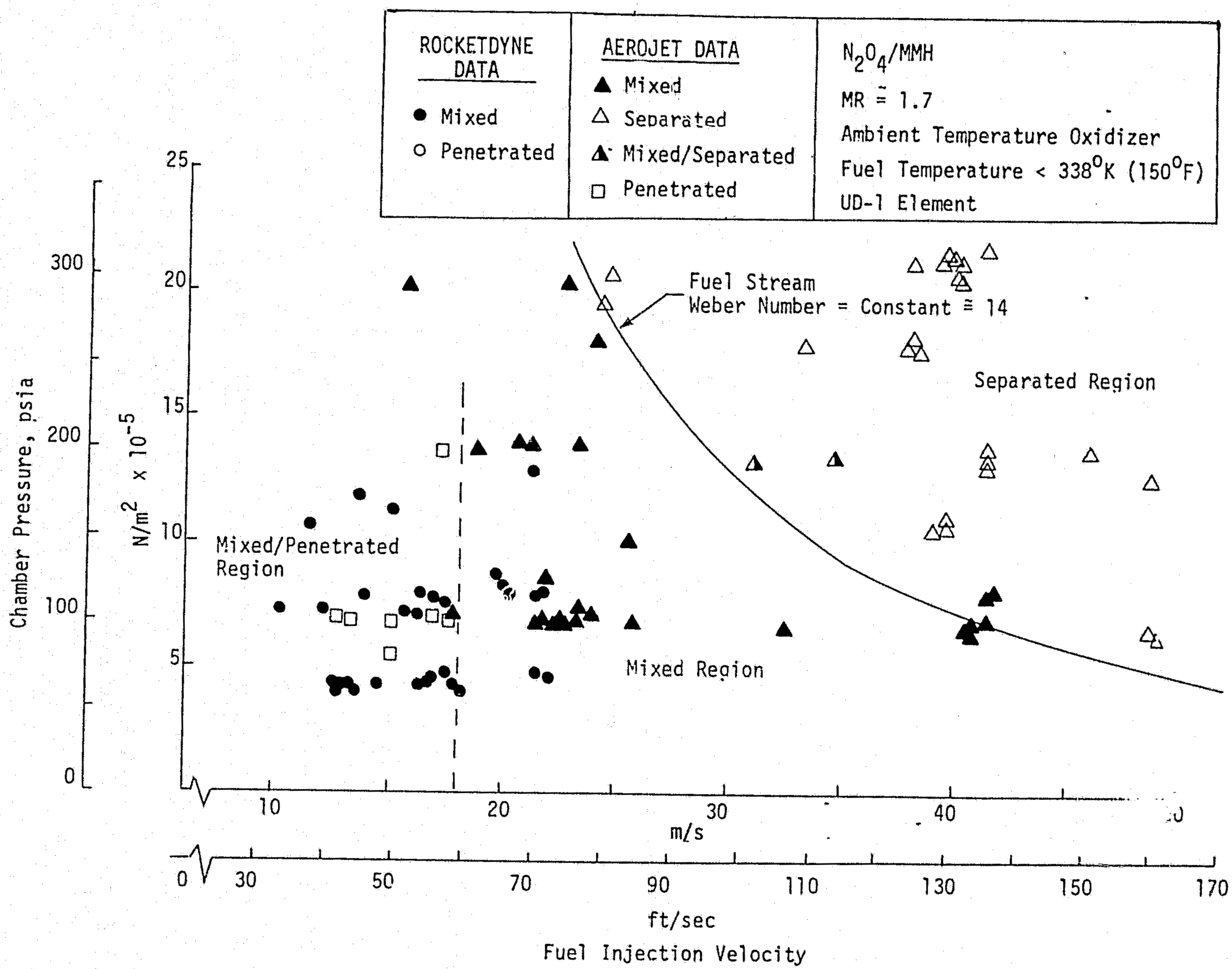

Figure 5-1. Correlation of Reactive Stream Separation to Chamber Pressure and Fuel Injection Velocity for UD-1 Element

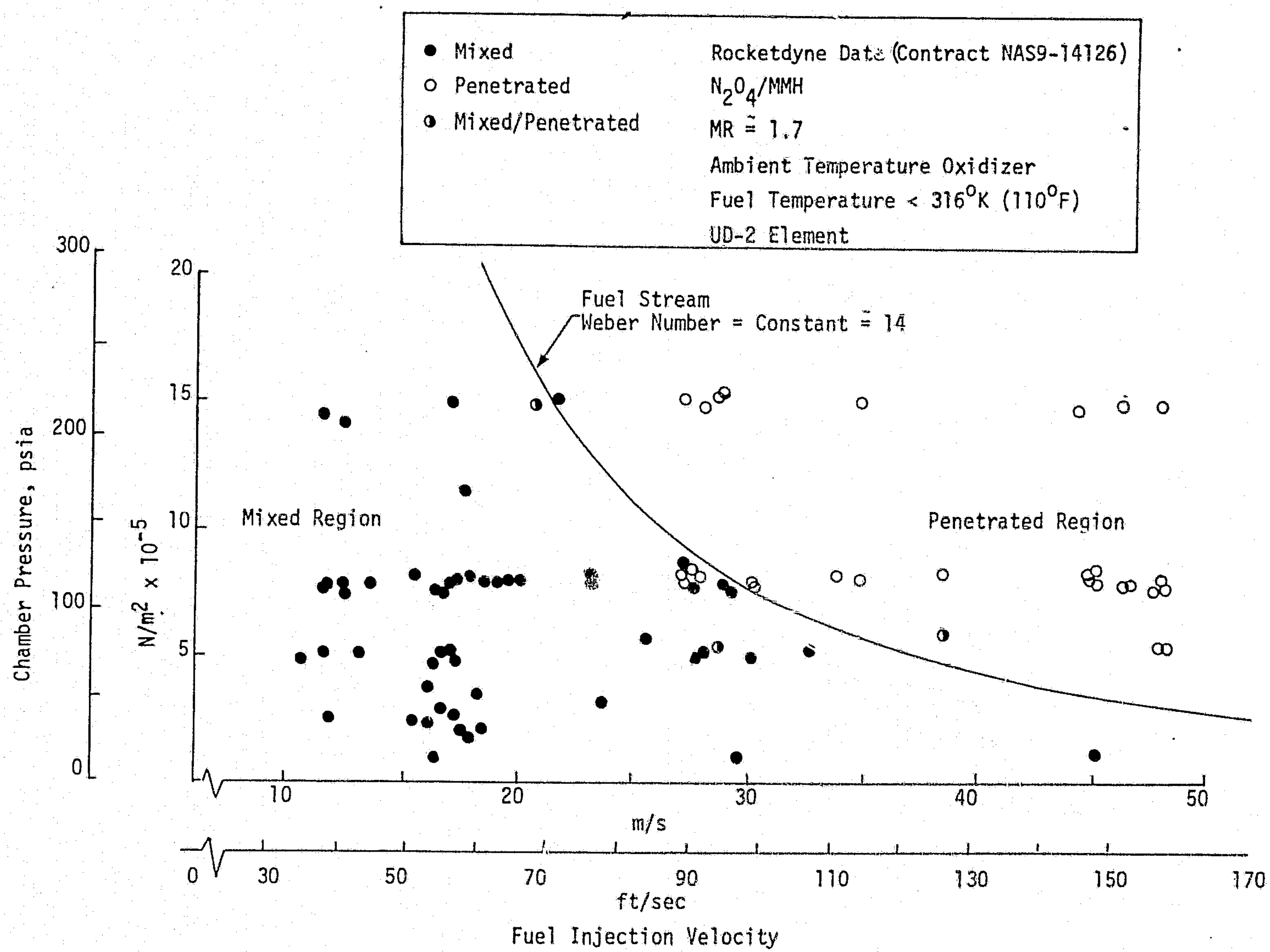

Figure 5-2. Correlation of Reactive Stream Separation to Chamber Pressure and Fuel Injection Velocity for UD-2 Element

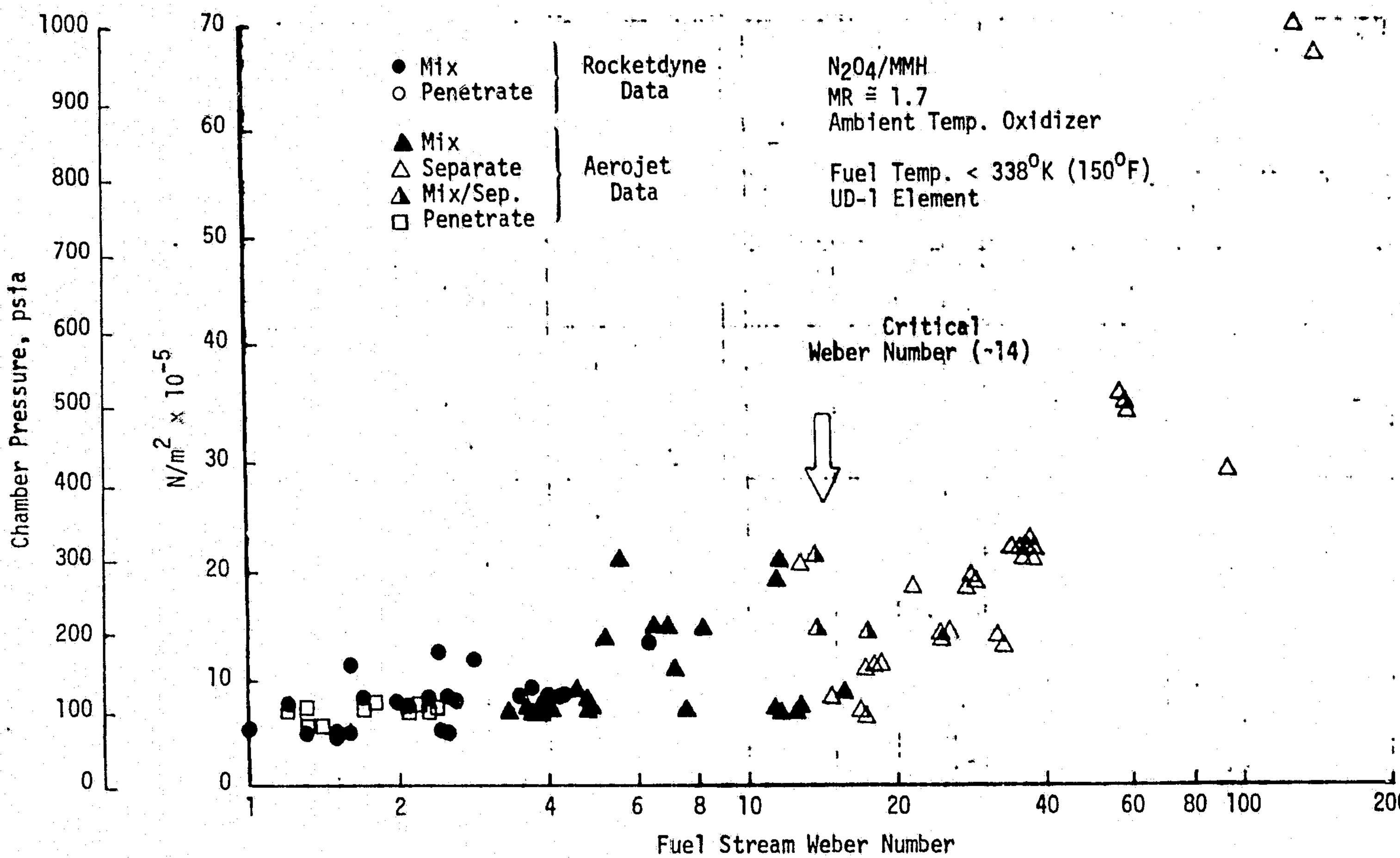

Figure 5-3. Correlation of Reactive Stream Separation to Fuel Stream Weber Number for UD-1 Element

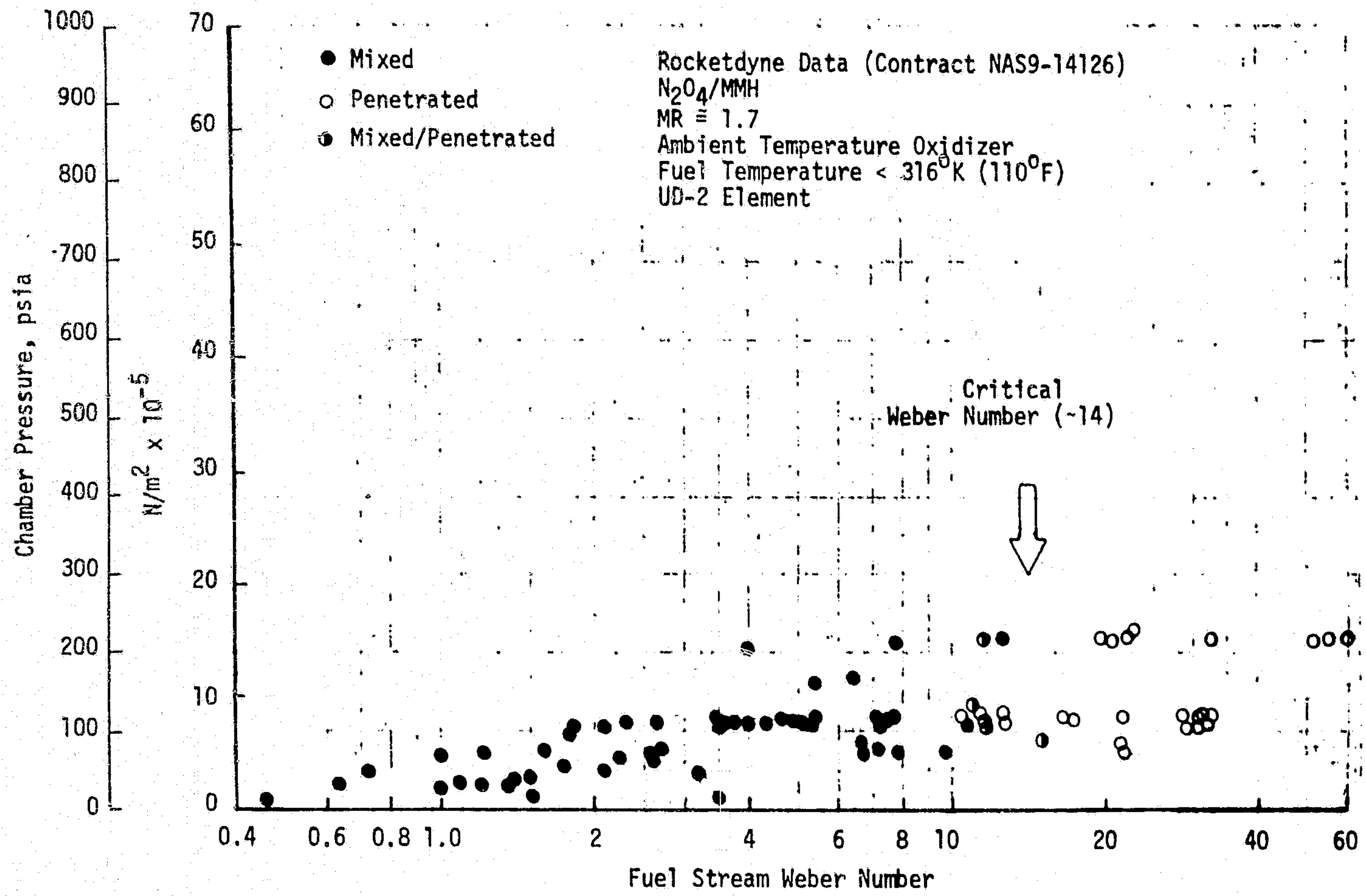

Figure 5-4. Correlation of Reactive Stream Separation to Fuel Stream Weber Number for UD-2 Element

the possible exception of whether the UD-1 element is mixed or penetrated at low injection velocities/Weber numbers. Reactive stream separation occurs above a critical Weber number of ~14 for both elements. Curves of constant fuel stream Weber number are shown in Figs. 5-1 and 5-2.

The Weber numbers shown plotted in Figs. 5-3 and 5-4 were calculated as follows:

$$\text{Weber No.} = \frac{\rho_g \, v_f^2 \, d_f}{\sigma_f \, g_c} \tag{5-1}$$

where

ρ_g = combustion gas density

v_f = fuel injection velocity

d_f = fuel orifice diameter

σ_f = surface tension of the fuel

g_c = gravitational constant $\left(32.174 \, \frac{\text{lbm}}{\text{lbf}} \cdot \frac{\text{ft}}{\text{sec}^2}\right)$

The gas density employed in the calculation of the Weber number was the combustion gas density at the injected mixture ratio. The Weber number is a ratio of aerodynamic-to-surface-tension forces for the jet.

The above correlation of data does not apply to tests conducted with fuel injection temperatures above the critical values noted in Figs. 5-1 and 5-2. That is, above fuel temperatures of 338°K (150°F) for the UD-1 element and 316°K (110°F) for the UD-2 element. Separation will occur above these temperatures for reasons to be explained later. Tests conducted with fuel temperatures above these critical values can exhibit separation at low Weber numbers (i.e., at Weber numbers <14).

As noted above, the phenomena observed at high injection velocites and chamber pressures with ambient temperature or moderately heated fuel was termed "penetration" by Rocketdyne and "separation" by Aerojet. The cause of the phenomena is not clear; however, several mechanisms have been proposed.

Aerojet (Ref. 26) has suggested that it may be due to high shear forces on the surface of the jet which causes some degree of self atomization, increased interfacial area and surface reactions and, thereby, separation. On the other hand, it may be due to the relative stability of the jets at high velocity.

A generalized correlation of the data for the UD-1 and UD-2 elements is presented in Fig. 5-5. Chamber pressure is shown plotted as a function of fuel injection velocity in this figure. Regions of mixing and reactive stream separation are noted. Note that the smaller element is less sensitive to chamber pressure and injection velocity effects (i.e., it is free from reactive stream separation over a greater range of P_c, v_f, and T_f).

It should be noted that since most of the tests were conducted at a nominal mixture ratio of ~1.7, a similar correlation could have been developed based on the oxidizer stream Weber number. Values of the oxidizer stream Weber number were approximately the same as for those of the fuel stream.

5.1.2 Heated Propellant Model

A heated propellant reactive stream separation model was developed based on both Rocketdyne's and Aerojet's data. The reactive stream separation phenomena occurring with heated propellants (termed separation) appeared to be different than the penetration phenomena observed at high injection velocities and chamber pressures with ambient temperature or moderately heated propellants.

Plots of chamber pressure versus fuel injection temperature for the UD-1 and UD-2 elements are presented as Figs. 5-6 and 5-7, respectively. A distinction as to whether each test is mixed, separated, or mixed/separated is made in the figures. Differentiation between Rocketdyne and Aerojet data is also made in Fig. 5-6. Tests with fuel stream Weber numbers greater than the critical value of ~14 and the low velocity penetrated tests reported by

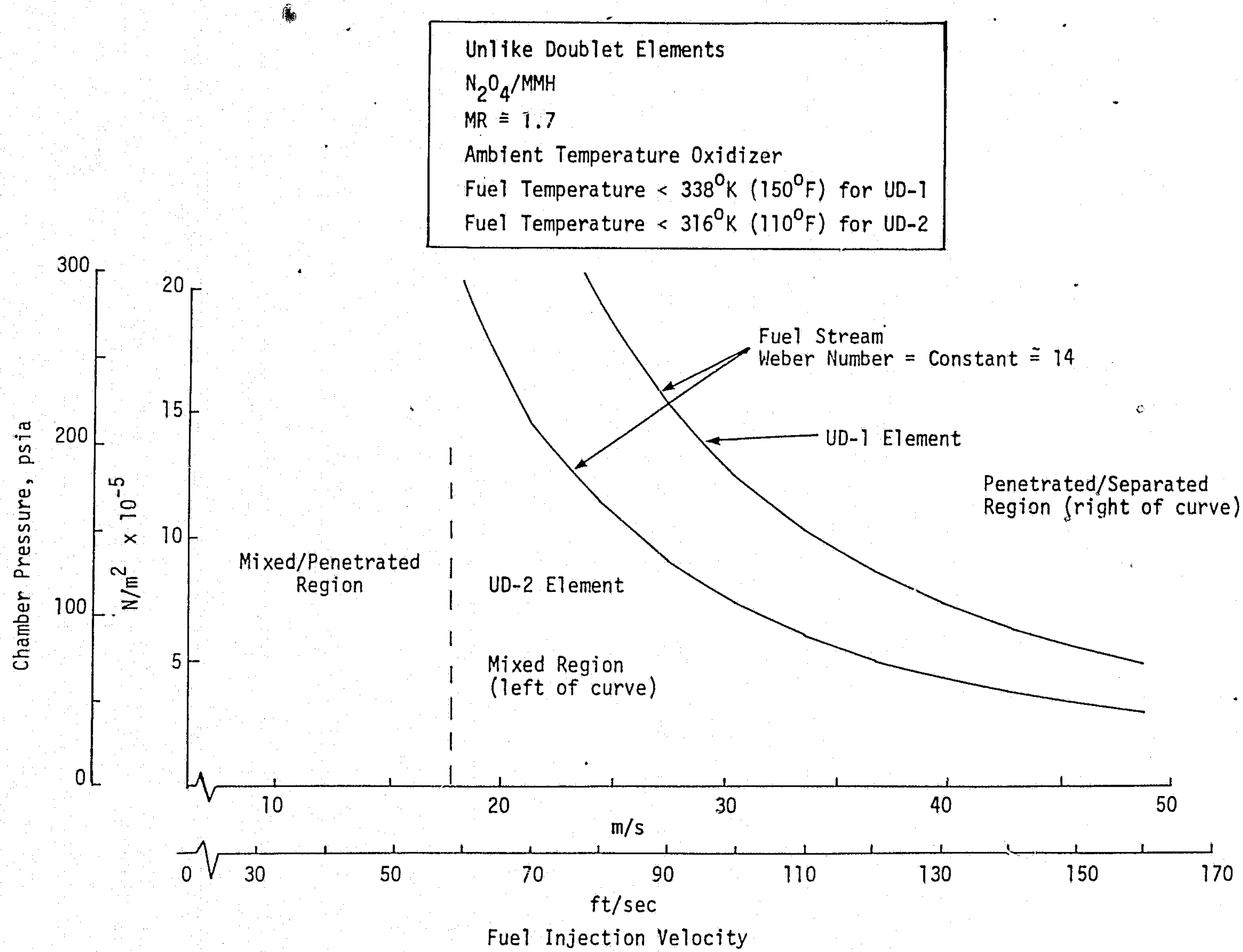

Figure 5-5. Generalized Correlation of Reactive Stream Separation to Chamber Pressure and Injection Velocity for Unlike Doublet Elements

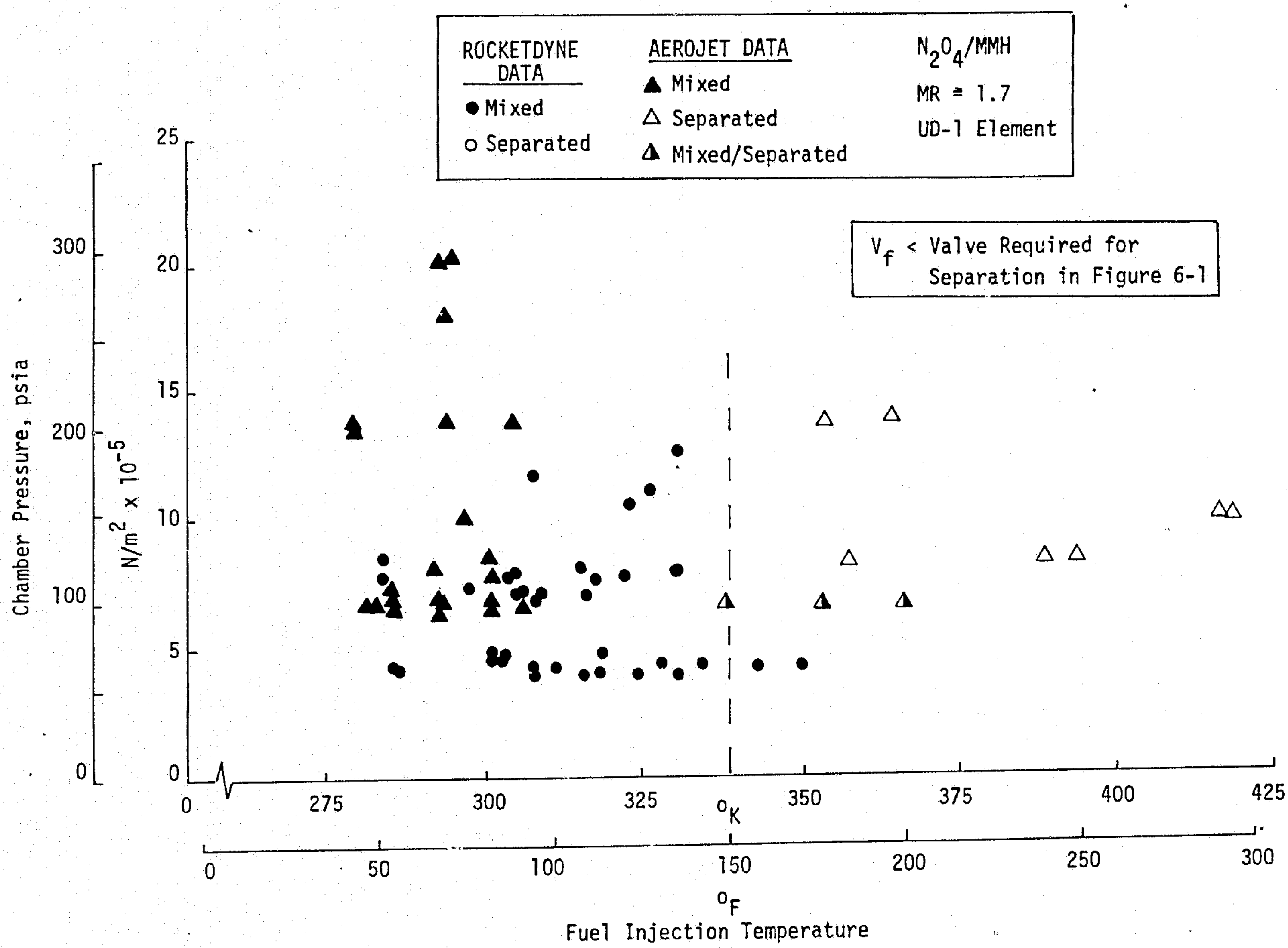

Figure 5-6. Correlation of Reactive Stream Separation to Chamber Pressure and Fuel Injection Temperature for UD-1 Element

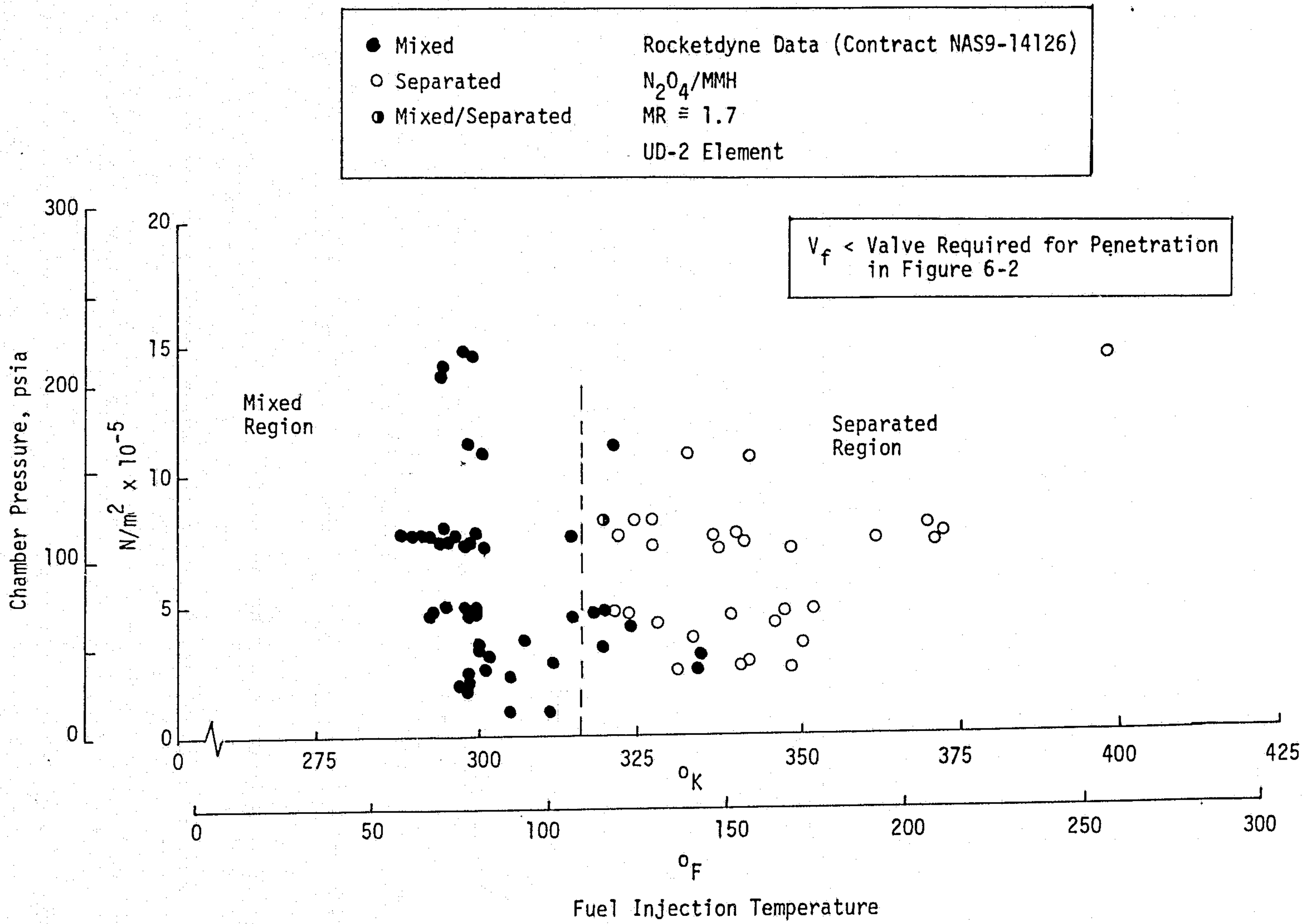

Figure 5-7. Correlation of Reactive Stream Separation to Chamber Pressure and Fuel Injection Temperature for UD-2 Element

Aerojet are not included on these plots. These data would only add confution to the analysis of fuel temperature effects on separation. The effect of fuel injection temperature on separation is quite evident. As would be expected from the method of data analysis (i.e., the method of defining tests as mixed, separated, or mixed/separated), which is qualitative and subjective, a clear cut maximum temperature without separation is not evident. However, it appears that in general separation occurs at fuel temperatures above ~338^{o}K (150^{o}F) with the UD-1 element and above ~316^{o}K (110^{o}F) with the UD-2 element. The larger element (i.e., the element with the larger orifice diameters) is more sensitive to the fuel injection temperature.

It should be noted that the data in Figs. 5-6/5-7 suggest that there may be an interaction of effects (chamber pressure and fuel temperature) on separation. The data suggests that it may be possible to operate at a higher fuel injection temperature at lower chamber pressures without separation.

<u>5.1.2.1 Derivation of Theoretical Model</u>. A theoretical model was developed to provide a more systematic basis for correlation of the heated fuel experimental reactive stream separation data to significant parameters. Formulation of this model was anticipated to provide insight into the significant parameters affecting separation and in turn lead to suggestions for the development of a better analytical model. Because available data indicate that energetic cyclic separation (popping) does not occur with the N_2O_4/MMH system over the range of element sizes investigated, the model does not provide for its description; however, addition

of this capability to a more generalized model can be made if warranted by future experimental results.

The theoretical model assumes that reactive stream separation occurs primarily thorugh the gas evolution resulting from a chemical reaction equivalent to that shown in Eq. (5-2).

$$CH_3NHNH_2 + N_2O_4 \rightarrow 2\ N_2 + 3\ H_2O + CO \tag{5-2}$$

The heat of reaction for process shown by Eq. (5-2) is approximately 7500 Btu/lbm of MMH reacted or approximately 5.7×10^4 Btu/lb mole of product gas formed. The reaction is assumed to occur very rapidly in a mixing zone within the doublet spray fan as shown in Fig. 5-8. The mixing zone originates at the jet impingement point and is assumed to grow linearly with downstream distance from this point until it completely fills the liquid sheet. The overall length of the sheet is L_c, the downstream distance at which it breaks up into droplets and ligaments. Intimate mixing of both mass and energy are assumed within the mixing zone, i.e., the heat from reaction is assumed to be absorbed principally by the unreacted liquids in the mixing zone and the product gas is in thermal equilibrium with the liquid.

The generation of blowapart-producing gas is assumed to follow a zero order reaction mechanism defined by the Arrhenius relation

$$\frac{d\ V_g}{dt} = \mathcal{R} = Ae^{-\Delta E/R_g T} \tag{5-3}$$

where V_g is the volume of gas generated per unit volume of mixed reaction zone, A is the zero order reaction rate constant (time^{-1}) and the remaining symbols have their usual meaning as defined in the Nomenclature section. With the usual transformation for flow problems

$$dt = \frac{1}{U}\ dx \tag{5-4}$$

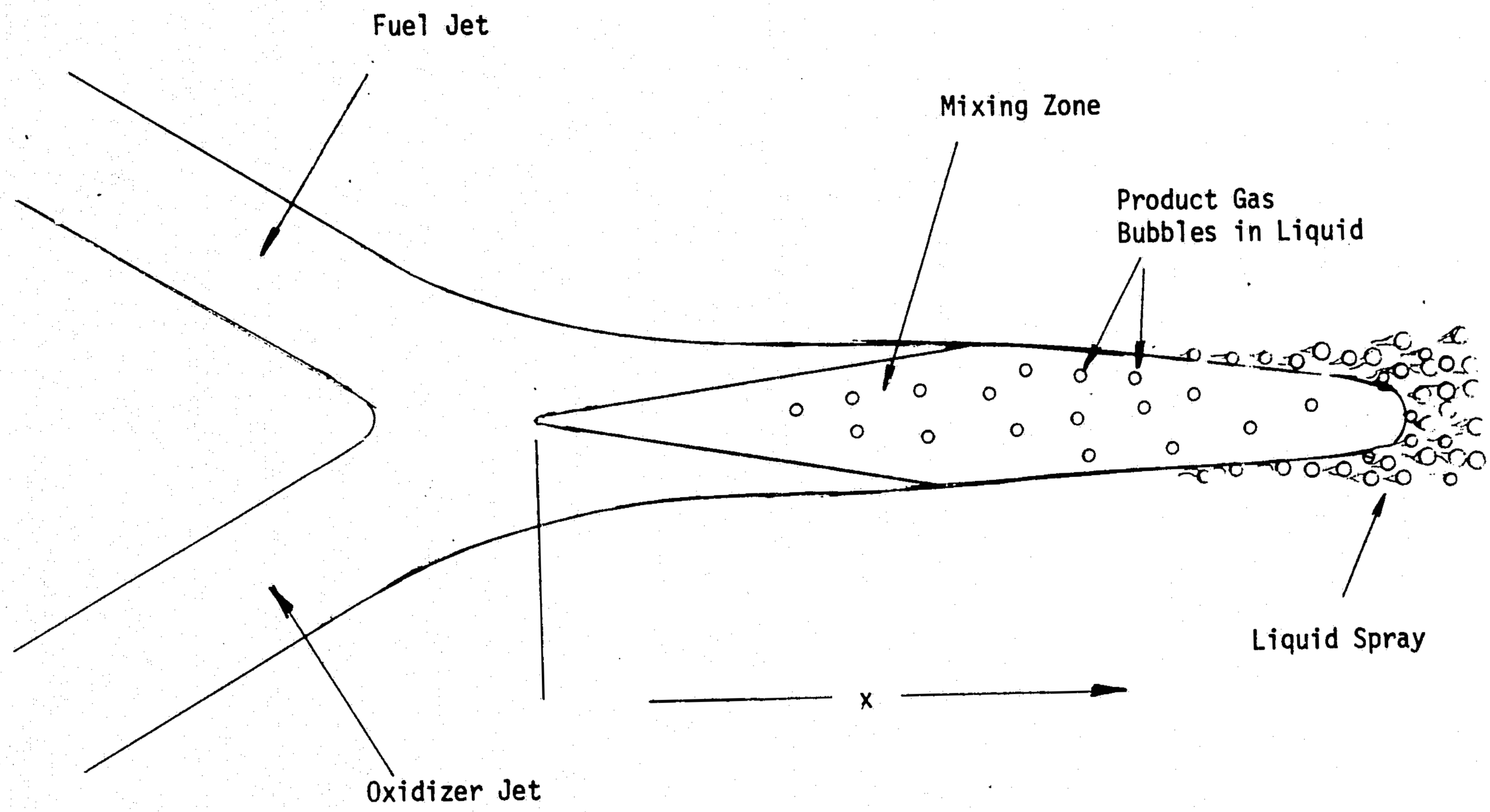

Figure 5-8. Doublet Sheet Model for Theoretical Analysis of Separation

Eq. (5-3) becomes

$$\frac{d\,V_g}{dx} = \frac{A}{U}\ e^{-\Delta E/R_g T} \tag{5-5}$$

The volumetric rate of heat generation is given by

$$\frac{dQ}{dt} = \rho_g\ \mathcal{R}\Delta H \tag{5-6}$$

Combining Eqs. (5-4), (5-5), and (5-6) gives

$$\frac{dQ}{dx} = \Delta H\ \rho_g\ \frac{Ae^{-\Delta E/R_g T}}{U} = \Delta H\ \rho_g\ \frac{\mathcal{R}}{U} \tag{5-7}$$

If the heat generated by the reaction is assumed to be absorbed by the liquid in the mixing zone with a resultant temperature rise, the temperature rise will, in turn, increase the reaction rate. Differentiating Eq. (5-3) with respect to temperature and then with respect to distance along the liquid sheet

$$\frac{d\mathcal{R}}{dT} = Ae^{-\Delta E/R_g T}\left(\frac{\Delta E}{R_g T^2}\right) = \mathcal{R}\left(\frac{\Delta E}{R_g}\right)\frac{1}{T^2}$$

$$\frac{d\mathcal{R}}{dx} = \frac{d\mathcal{R}}{dT}\ \frac{dT}{dx} = \left(\frac{\Delta E}{R_g T^2}\right)\mathcal{R}\ \frac{dT}{dx} \tag{5-8}$$

The analysis presented in Appendix A indicates that the total reaction required to produce a blowapart condition is a very small fraction of the total flow. This also indicates that the temperature rise in the mixed reaction zone can be assumed to be a small fraction of the absolute temperature which can be approximated by a mean temperature in the term $(\Delta E/R_g T^2)$. Defining

$$K_1 = \Delta E/R_g\overline{T}^2 \cong \Delta E/R_g\ T_o^{\ 2}$$

$$\frac{d\mathcal{R}}{dx} = K_1\mathcal{R}\ \frac{dT}{dx} \tag{5-9}$$

But

$$\frac{dT}{dx} = \frac{1}{C_p\ \rho_L}\ \frac{dQ}{dx} = \frac{\Delta H}{C_p}\left(\frac{\rho_g}{\rho_L}\right)\ \frac{\mathcal{R}}{U} \tag{5-10}$$

Combining Eq. (5-9) and (5-10), and re-arranging

$$\frac{d\mathcal{R}}{\mathcal{R}^2} = \frac{\Delta H}{C_p}\left(\frac{\rho_g}{\rho_L}\right)\frac{K_1}{U}\ dx \tag{5-11}$$

Integrating and re-arranging

$$\mathcal{R} = \frac{\mathcal{R}_o}{1 - \frac{\Delta H}{C_p\ T_o^{\ 2}}\left(\frac{\rho_g}{\rho_L}\right)\left(\frac{\Delta E}{R_g}\right)\left(\frac{x}{U}\right)\mathcal{R}_o} \tag{5-12}$$

By assuming the genrated gas in the reaction zone to be in thermal equilibrium with the liquid, which is in turn close to the impingement point temperature T_o, the gas density can be approximated by

$$\rho_g = \frac{P}{R_g\ T_o}$$

Therefore,

$$\mathcal{R} = \frac{\mathcal{R}_o}{1 - \frac{\Delta H}{C_p\ T_o^{\ 3}}\left(\frac{P}{\rho_L}\right)\frac{\Delta E}{R_g^{\ 2}}\left(\frac{x}{U}\right)\mathcal{R}_o} \tag{5-13}$$

The functional relation between gas generation rate $\mathcal{R}$ and x shown in Eq. (5-13) defines a critical distance x_c at which the gas generation reaches a critical value $\mathcal{R}_c$. Re-arranging Eq. (5-13) to solve for x_c gives

$$x_c = \frac{U\,T_o^{\,3}}{\left(\frac{\Delta H}{C_p}\right)\left(\frac{P}{\rho_L}\right)\left(\frac{\Delta E}{R_g^{\,2}}\right)\mathcal{R}_c}\left[\frac{\mathcal{R}_c}{\mathcal{R}_o} - 1\right]$$

To develop a useful correlation, the critical reaction length x_c is divided by a critical hydrodynamic length L_c, defined as being the point at which the spray fan has spread sufficiently that blowapart cannot occur. The most obvious choice for L_c is the ligament length (i.e., the distance downstream of the impingement point at which the liquid breaks up into droplets and ligaments). This distance is defined by

$$L_{c_1} = C_1 \frac{D}{U} \qquad (5\text{-}14)$$

where C_1 has a value of 61 m/sec (200 ft/sec) for water jets of equal diameter (Ref. 9). However, photographic studies conducted at Rocketdyne have indicated that for injection velocities and orifice diameters similar to those of this study this distance is approximately one jet diameter, i.e.,

$$L_{c_2} = D \qquad (5\text{-}15)$$

It may, however, be that the mixing length which has been observed to be proportional to the jet diameter, i.e.,

$$L_{c_3} = C_3 D \qquad (5\text{-}16)$$

where $C_3 \cong 2$ (Ref. 9) should be employed.

Development of equations and attempts to correlate the data were carried out using each of the above equations to define L_C. In general, data for either element could be correlated well by substitution of an expression for L_C that was proportional to the jet diameter (i.e., Equations 5-15/5-16) into Eq. (5-13). However, to collapse the data for both elements to a single correlation it was necessary to consider L_C as a constant. Considering the size of the elements and range of injection velocities studied, this assumption does not seem illogical. A value for L_C equal to the mean diameter of the elements orifices was employed in the final correlation of the data, i.e.,

$$L_{C_4} = 0.07430 \text{ cm } (0.02925\text{-inch}) = C_4 \tag{5-17}$$

Development of the equation used to correlate the data will be carried out using Eq. (5-17) to define L_C. Equation (5-13) becomes

$$\frac{x_c}{L_C} = \frac{U\, T_o^{\,3}}{C_4\, P \left(\frac{\Delta H}{C_p\, \rho_L}\right)\left(\frac{\Delta E}{R_g^{\,2}}\right) \mathcal{R}_c} \left[\frac{\mathcal{R}_c}{\mathcal{R}_o} - 1\right] \tag{5-18}$$

Equation (6-18) can be divided into dimensionless groups as follows:

$$\left(\frac{x_c}{L_C}\right) = \left[\frac{U\, T_o^{\,2}\, C_p\, \rho_L\, R_g}{C_4\, P\, \Delta H\, \mathcal{R}_c}\right] \left(\frac{R_g\, T_o}{\Delta E}\right) \left[\frac{\mathcal{R}_c}{\mathcal{R}_o} - 1\right] \tag{5-19}$$

The critical reaction rate $\mathcal{R}_c$ (volume/volume time) is expected to be proportional to the velocity, U, i.e.,

$$\mathcal{R}_c = BU \tag{5-20}$$

Equation (5-19) becomes

$$\left(\frac{x_c}{L_c}\right) = \left[\frac{T_o^{\,2}\, C_p\, \rho_L\, R_g}{C_4\, B\, P\, \Delta H}\right] \left(\frac{R_g\, T_o}{\Delta E}\right) \left[\frac{BU}{\mathcal{R}_o} - 1\right] \tag{5-21}$$

with

$$\mathcal{R}_o = A e^{-\Delta E/R_g T_o} \tag{5-22}$$

Mixing occurs when (x_c/L_c) is greater than unity. Separation is predicted to occur for (x_c/L_c) less than unity. Evaluation of required constants B, A, and ΔE must be made by correlation of appropriate experimental data.

<u>5.1.2.2 Model Correlation.</u> Although Eq. (5-21) is in non-dimensional form, it contains dimensional coefficients B, ΔE and A which are dimensional and are initially unknown. To correlate the experimental data to the model, Eq. (5-21) is first re-arranged as follows:

$$\left(\frac{x_c}{L_c}\right) \left[\frac{T_o^{\,3}\, C_p\, \rho_L\, R_g^{\,2}}{C_4\, P\, \Delta H}\right]^{-1} = \left(\frac{1}{B\Delta E}\right) \left[\frac{BU}{A}\, e^{\Delta E/R_g T_o} - 1\right] \tag{5-23}$$

so that the known and unknown parameters have been separated into new non-dimensional groups. It can now be noted that when

$$\frac{BU}{A}\, e^{\Delta E/R_g T_o} \leqq 1$$

the doublet must be separated because the reaction rate at the impingement point is already greater than the critical rate. The operating regime of interest (particularly for purposes of correlation) occurs when

$$\frac{BU}{A}\, e^{\Delta E/R_g T_o} - 1 \sim \frac{BU}{A}\, e^{\Delta E/R_g T_o}$$

In this case, Eq. (5-23) becomes

$$\left(\frac{x_c}{L_C}\right)\left[\frac{U\ T_o^{\ 3}\ C_p\ \rho_L\ R_g^{\ 2}}{C_4\ P\ \Delta H}\right]^{-1} = \frac{1}{\Delta EA}\ e^{\Delta E/R_g\ T_o} \tag{5-24}$$

Although the value of (x_c/L_C) during a given hot firing experiment is unknown, it is known that

$x_c/L_C < 1$ gives separation

$x_c/L_C > 1$ gives mixing

$x_c/L_C = 1$ is the boundary between separation and mixing

Rocketdyne's hot firing data with the UD-1 and UD-2 elements together with the data of Aerojet with the UD-1 element were correlated by plotting

$$\left[\frac{U\ T_o^{\ 3}\ C_p\ \rho_L\ R_g^{\ 2}}{C_4\ P\ \Delta H}\right]^{-1} \quad \text{versus } 1/T_o$$

on semilog paper with

$C_4 = 0.02925$-inch

$U = v_f$

$$P = P_c + \frac{\rho_L\ v_f^{\ 2}}{2g}$$

$T_o = T_{Inj}$ of the hotter propellant

It should be noted that as long as ϕ is near unity the effect of using v_f for U will be compensated by a change in the eventual definitions of B and A. The results of the correlations are presented in Fig. 5-9. Aerojet's low velocity penetration tests and those tests for which reactive stream separation is indicated by the Impinging Jet Characteristics Model are not included in the data correlation. The plot shows a reasonable correlation of the data in view of the qualitative and subjective means of determining mixed versus separated test conditions.

If the boundary between the separated and mixed regions is assumed to be that shown by the line in Fig. 5-9, then the slope of the line defines a value for the activation energy ΔE of 13.0×10^6 ft lb/lb mole. With this value of ΔE, a value of 1.7×10^{10} sec^{-1} was calculated for the frequency factor A. It is important to note that these values are reasonable for these propellants.

With values of ΔE and A defined, Eq. (5-24) can be rearranged as follows to provide a design criteria to prevent separation. That is,

$$\boxed{\frac{x_c}{L_c} = \frac{1}{\Delta EA} e^{\Delta E/R_g T_o} \left[\frac{U T_o^3 C_p \rho_\ell R_g^2}{C_4 P \Delta H} \right] > 1} \qquad (5\text{-}25)$$

The value of all quantities required to calculate x_c/L_c are known.

It is believed that the correlation of data obtained with the above model provides insight into the significant parameters affecting separation and can in turn lead to suggestions for the development of a better analytical model.

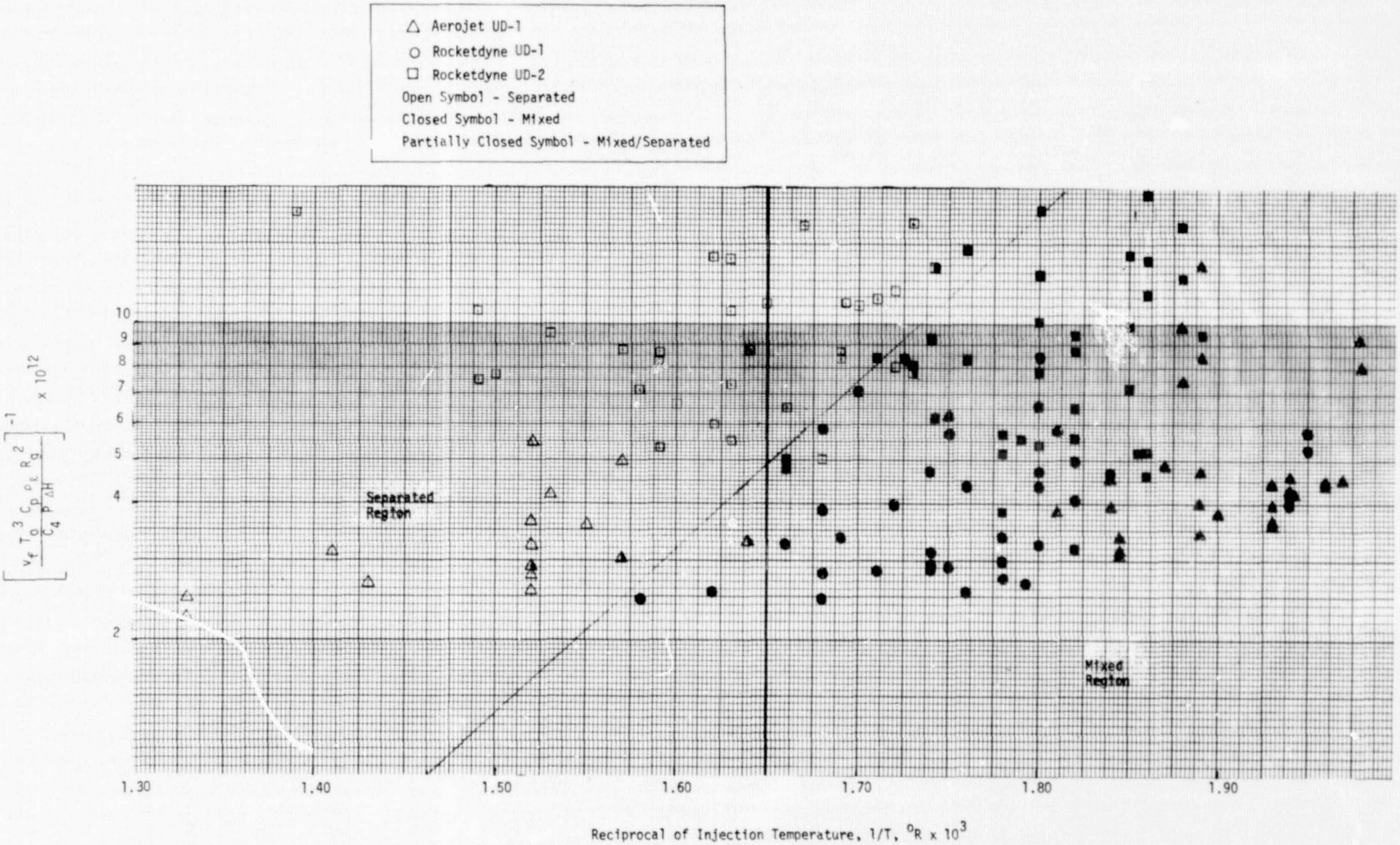

Figure 5-9. Correlation of Experimental Data According to Model of Equation (5-24)

5.2 DESIGN CRITERIA

The data correlations presented in the previous section of this report (Section 5.1) provide design criteria (guidelines) which will allow for the design of stable high performing injectors that are free from reactive stream separation. Since two different types of reactive stream separation, with different driving mechanisms, were observed, two reactive stream models were developed. Each of the models define a design criteria that should be employed in the design of an injector to ensure that it is free from reactive stream separation.

To prevent penetration, the design criteria established by the Impinging Jet Characteristics Model (Section 5.1.1) should be employed. That is, the injector should be designed with

$$\boxed{\text{Weber Number} = \frac{\rho_g \, v_f^{\,2} \, d_f}{\sigma_f \, g_c} < 14} \tag{5-26}$$

To prevent separation which can occur with heated propellants, the design criteria established from the Heated Propellant Model (Section 5.1.2) should be employed. That is, the injector should be designed according to the following criteria.

$$\boxed{\frac{X_c}{L_c} = \frac{1}{\Delta EA} \, e^{\Delta E/R_g T} \left[\frac{v_f \, T_o^{\,3} \, C_p \, \rho_\ell \, R_g^{\,2}}{C_4 \, P \, \Delta H} \right]}$$

where

$$\frac{x_c}{L_C} < 1 \quad \text{gives separation}$$

$$\boxed{\frac{x_c}{L} > 1 \quad \text{gives mixing}}$$

$$\frac{x_c}{L_C} = 1 \quad \text{is the boundary between separation and mixing}$$

where

$\Delta E = 13.0 \times 10^6$ ft lb/lb mole

$A = 1.7 \times 10^{10}$ sec^{-1}

$C_4 = 0.02925$-inch

The value of all quantities required to calculate x_c/L_C are known.

6.0 CONCLUDING REMARKS AND RECOMMENDATIONS

The objectives of this study were: (1) to develop an understanding of the mechanisms that cause reactive stream separation for hypergolic propellants, and (2) through a basic understanding of the governing mechanisms, establish design criteria which would allow for the design of stable high performing injectors that are free from reactive stream separation. These objectives were achieved.

The investigation was limited to the N_2O_4/MMH propellant combination, unlike-doublet-type element, and to a range of operating conditions applicable to the Space Tug and Space Shuttle attitude control and maneuvering engines. Use of the design criteria established herein for other propellant combinations or element types is not recommended; however, the experimental technique employed and basic understanding of the phenomenon occurring could be applied to establish design criteria for other propellant combinations and/or other element types.

From the experimental data obtained it was concluded that two different types of reactive stream separation, with different driving mechanisms, were observed. One of these, termed penetration, was observed at high injection velocities and/or chamber pressures with ambient temperature or moderately heated (fuel) propellants. The other phenomena, termed separation, occurred at elevated fuel temperatures. In both cases, the observed reactive stream separation phenomenon consisted of repeated pulses (i.e., it was cyclic). However, the pulsing did not exhibit the strength necessary to either disrupt the doublet jets upstream of the impingement point or to completely destroy the spray fan downstream of the impingement point; i.e., there were no instances of energetic stream blowapart or "popping" observable in the film data. The frequency of the cycle phenomenon was on the order of 10 to 20 cycles per second.

It is further concluded that the tendency toward reactive stream separation increases with increasing fuel injection temperature, element orifice size,

chamber pressure, and propellant injection velocity. The results of this investigation suggest that if an unlike-doublet element injector is employed for the application investigated (i.e., Space Tug and Space Shuttle attitude control and orbital maneuvering engines) small element orifice diameters and/or moderate fuel injection temperatures will be required to ensure operation in a regime without reactive stream separation.

Specifically, the following recommendations for future effort are:

1. Investigate the use of other element types such as like doublets and/or triplets.
2. Study other propellant combinations such as N_2O_4/50-50 and/or ClF_3/MMH.
3. Conduct further studies with the unlike-doublet element and investigate more thoroughly the effects of orifice size and jet stability characteristics.

If further studies of this nature are conducted, serious consideration should be given to the possible use of a more quantitative measure of reactive stream separation. The method of determining reactive stream separation in this study was qualitative and subjective; however, the results obtained were consistent with those of the related effort conducted by Aerojet (Contract NAS9-14186).

7.0 REFERENCES

1. Elverum, G. W., Jr., and P. Staudhammer: The Effect of Rapid Liquid-Phase Reactions on Injector Design and Combustion in Rocket Motors, Progress Report 30-4, Jet Propulsion Laboratory, Pasadena, California, August 1959.

2. Johnson, B. H.: An Experimental Investigation of the Effects of Combustion on the Mixing of Highly Reactive Liquid Propellants, Technical Report 32-689, Jet Propulsion Laboratory, Pasadena, California, July 1965.

3. Stanford, H. B., and W. H. Tyler: "Injector Development", Supporting Research and Advanced Development, Space Programs Summary 37-51, Vol. IV, Jet Propulsion Laboratory, Pasadena, California, February 1965, p. 192.

4. Stanford, H. B.: "Injector Development," Supporting Research and Advanced Development, Space Programs Summary 37-36, Vol. IV, Jet Propulsion Laboratory, Pasadena, California, December 1965, p. 174.

5. Riebling, R. W.: "Injector Development; Stream Separation Experiments," Supporting Research and Advanced Development, Space Program Summary 37-45, Vol. IV, Jet Propulsion Laboratory, Pasadena, California, 30 June 1967.

6. Riebling, R. W.: "Injector Development; Stream Separation Experiments," Supporting Research and Advanced Development, Space Program Summary 37-45, Vol. IV, Jet Propulsion Laboratory, Pasadena, California, 30 June 1967.

7. Woodward, J. W.: "Combustion Effects in Sprays," Supporting Research and Advanced Development, Space Programs Summary 37-36, Vol. IV, Jet Propulsion Laboratory, Pasadena, California, December 1965.

8. Burrows, M. C. (NASA-Lewis Research Center): Mixing and Reaction Studies of Hydrazine and Nitrogen Tetroxide Using Photographic and Spectral Techniques, AIAA Paper No. 67-107, presented at the AIAA 5th Aerospace Science Meeting, New York, N. Y., January 1967.

9. Lawver, B. R., and B. P. Breen: Hypergolic Stream Impingement Phenomena - Nitrogen Tetroxide/Hydrazine, NAS-CR-72444, Dynamic Science Division, Marshall Industries, Monrovia, California, October 1968.

10. Zung, L. B. (Dynamic Science Corporation, Monrovia, California): Hypergolic Impingement Mechanisms and Criteria for Jet Mixing or Separation, presented at the 6th ICRPG Liquid Propellant Combustion Instability Conference, 9-11 September 1969.

11. R-7223: Reactive Stream Impingement, Rocketdyne, a division of Rockwell International, 29 September 1967.

12. Houseman, J. (Jet Propulsion Laboratory, Pasadena, California): Jet Separation and Optimum Mixing for an Unlike Doublet, presented at the 6th ICRPG Liquid Propellant Combustion Instability Conference, 9-11 September 1969.

13. Campbell, D. T., Photographic Study of Hypergolic Propellant Stream Blowapart, presented at AIAA Joint Specialists Conference, San Diego, California, 1970.

14. Kushida, R., and J. Houseman: Criteria for Separation of Impinging Streams of Hypergolic Propellants, JPL Report WSCI-67-38, 1967.

15. Wuerker, R. F., B. J. Matthews, and R. A. Briones (TRW Systems Group): Producing Holograms of Reacting Sprays in Liquid Propellant Rocket Engines, TRW Report 68.4712.2-024, 31 July 1968.

16. Lee, A., and J. Houseman: Popping Phenomena with N_2O_4/N_2H_4 Injectors, presented at the Western States Section Meeting of the Combustion Institute on Stable Combustion of Liquid Propellants, JPL, October 26-27, 1970.

17. Clayton, R.: Experimental Observations Relating the Inception of Liquid Rocket Engine Popping and Resonant Combustion to the Stagnation Dynamics of Injection Impingement, TR 32-1479, JPL, 15 December 1970.

18. Perlee, H., et al.: Hypergolic Ignition and Combustion Phenomena in the Propellant System Aerozine - 50/N_2O_4, Final Report No. 4019, Bureau of Mines, Pittsburgh, Pennsylvania, April 1, 1965 to March 31, 1967.

19. Friedman, R., et al.: A Study of Explosions Induced by Contact of Hydrazine-type Fuels with Nitrogen Tetroxide, Technical Document ASD-TDR-62-685, Atlantic Research Corporation, September 1962.

20. Rodriguez, S., and A. Axworthy: Liquid Phase Reactions of Hypergolic Propellants, R-8374, Rocketdyne, a division of Rockwell International, Canoga Park, California, December 1970.

21. Nurick, W., and J. Cordill: Reactive Stream Separation Photography, Final Report, R-8490, Rocketdyne, a division of Rockwell International, Canoga Park, California, May 1972.

22. Lawver, B. R.: Rocket Engine Popping Phenomena, Aerojet General Report No. TCER 9642:0095, March 1969.

23. Houseman, J.: Jet Separation and Popping with Hypergolic Propellants, presented at the 7th JANNAF Combustion Meeting, CPIA Publication 204, Vol. 1, February 1971, pp 445-453.

24. Lawver, B. R.: A Model of the Hypergolic Pop Phenomena, J. Spacecraft and Rockets, Vol. 9, No. 4, April 1972, pp 225-226.

25. Rupe, J. H., A Correlation Between the Dynamic Properties of a Pair of Impinging Streams and the Uniformity of Mixtu e Ratio Distribution in the Resulting Spray, Progress Report No. 20-209, Jet Propulsion Laboratory, Pasadena, Calif., 28 March 1956.

26. Lawver, B. R., High Performance N_2O_4/Amine Elements -"Blowapart", Task III Data Dump, Contract NAS9-14186, Report 14186-DR6-3-1, Aerojet Liquid Rocket Company, 15 November 1974.

8.0 NOMENCLATURE

A	Zero order reaction rate constant (sec^{-1})
B	Critical rate coefficient (ft^{-1})
C_p	Specific heat of liquid (Btu/lb ^oR)
C_1	Critical sheet length coefficient (200 ft/sec)
C_2	Critical mixing zone coefficient (2)
d	Orifice diameter
D	Mean jet diameter (ft)
ΔE	Activation energy (lbf-ft/lb mole ^oR)
ΔH	Heat of reaction (Btu/lb mole gas)
K_1	Lumped coefficient for integration
L_C	Critical hydrodynamic length (ft)
MR	Mixture ratio ($\dot{W}_{ox}/\dot{W}_f$)
P	Pressure in fan (lbf/ft^2)
P_c	Chamber pressure (lbf/ft^2)
Q	Volumetric heat generation (Btu/ft^3)
Ω	Reaction rate volume/volume-sec
R_g	Gas constant (1544 lbf ft/lb mole ^oR)
T	Temperature (^oR)
t	Time (sec)
U	Fan velocity (ft)
v	Injection velocity

V	Specific volumetric gas generation (volume/volume)
$\dot{W}$	Flowrate
x	Distance along fan (ft)
ρ_g	Density of gas (lb mole/ft^3)
ρ_ℓ	Density of liquid (lb/ft^3)
ϕ	Mixing index

<u>Subscript</u>

c	Critical
g	Gas
ℓ	Liquid
o	At impingement point
f	Fuel
ox	Oxidizer

9.0 APPENDIX A

ESTIMATION OF CHEMICAL REACTION NECESSARY TO PRODUCE SEPARATION

To calculate a critical chemical reaction rate, one first estimates the density ratio (ρ_g/ρ_L) in the spray fan mixing zone. If this ratio is large, the percent reaction required to violently expand the fan (blowapart) is small. By the ideal gas law

$$\rho_g = \frac{\overline{MW}}{359} \left(\frac{P}{14.7}\right) \left(\frac{460}{T}\right) \qquad \text{(A-1)}$$

From Equation (5-2)

$$\overline{MW} = \frac{2(28) + 3(18) + 28}{2 + 3 + 1} = 23$$

For applications similar to the OME thrust chamber, a pressure of 10 atm (147 psia) provides an appropriate example. Although the gas temperature is difficult to define, the proposed theoretical model assumes it to be in equilibrium with the surrounding liquid. A temperature of 600°R can therefore be assigned. Then, from Equation (A-1),

$$\rho_g = \left(\frac{23}{359}\right)\left(\frac{14.7}{14.7}\right)\left(\frac{460}{600}\right) = .489 \text{ lb/ft}^3$$

For a mixture ratio (MR) of 1.6, the liquid density is given by

$$\rho_L = \frac{1 + MR}{\frac{1}{\rho_{MMH}} + \frac{MR}{\rho_{N_2O_4}}} = \frac{1 + 1.6}{\frac{1}{55} + \frac{1.6}{90}} \cong 72 \text{ lb/ft}^3$$

$$\rho_g/\rho_L = \frac{.489}{72} = .0067$$

If only .0067 (approximately 1/2 percent) of the liquid propellants react in the liquid sheet, the gas formed will occupy the same volume as the total reacting liquids. A blowapart condition therefore requires only a very small fraction of the liquid propellants to react.